THE STATUS OF THE STANFORD LINEAR COLLIDER*

RAE STIENING
Stanford Linear Accelerator Center
Stanford University, Stanford, California 94305

1. Introduction

It has been recognized for some time that the extension of conventional electron-positron storage rings to energies higher than a few hundred GeV is very difficult because of the rapid increase with energy of synchrotron radiation in the ring bending magnets. An alternate strategy for the production of high energy collisions is the linear collider in which the collisions are achieved without the need for such bending magnets. Although synchrotron radiation is a problem even in linear colliders because of the interaction between the beams at the collision point, this problem is not fundamental; there are several ways of changing the strength of the beam-beam interaction without changing the area of the interaction point and hence the luminosity.

The SLC project, which first received funding in 1983, is intended to be the first test of linear collider technology. Fortunately the (then postulated) existence of the Z particle, having a mass of 93 GeV and a unitarity saturating cross section, made it possible to design a test-of-concept linear collider which would satisfy valuable particle science objectives as well.

The accomplishments reported on in this paper are the result of the efforts of a large number of persons. No attempt has been made herein to refer to individuals or to cite published or unpublished documents. Many of the results summarized here are reported in more detail in numerous reports at this Conference.

The construction of the SLC was completed in March, 1987, at a total cost of just under 115.4 million dollars. Since February, 1986, various parts of the project have been commissioned. The initial commissioning luminosity goal is 6×10^{27}/cm²-sec. At this luminosity the production rate of Z particles is 15/day. When this luminosity goal is reached a detector will be placed around the interaction region and running for particle science purposes will begin. It is presently anticipated that this running will start on June 15. Table 1 shows the values of the SLC design parameters and the approximate values which will yield the initial luminosity goal.

2. Project Description

An overall layout of the SLC is shown in Fig. 1. Two 20 cm long bunches of electrons are emitted from a gated thermionic gun and accelerated to 160 keV. The bunches pass through two 178 MHz RF cavities and drift spaces and are compressed in length. Final compression is accomplished in a section of 2.8 GHz cavities. After passing through these cavities the bunches have been compressed to an rms length of about 2 mm each. The short bunches are accelerated in a linear accelerator to 200 MeV. At this point the two electron bunches are joined by a 200 MeV positron bunch and all three bunches are accelerated to 1.2 GeV. A splitter magnet deflects the electron bunches into a storage ring where their transverse emittance is damped by synchrotron radiation. The positron bunch is deflected into a different storage ring where its transverse emittance is also damped. After a time interval of 5.5 mS or longer, depending on the accelerator repetition rate, the positron bunch is extracted from the positron storage ring. Approximately sixty nanoseconds later the first of the two electron bunches in the electron storage ring is extracted. Sixty nanoseconds later the second electron bunch is also extracted.

Table 1. Basic Parameter Specifications

	Design Goal	Initial Goal	Achieved	Units
Beam Energy at IP	50	46	46	GeV
Beam Energy at End of Linac	51	47	53	GeV
Electrons at Entrance of Arcs	7×10^{10}	10^{10}	2.5×10^{10}	
Positrons at Entrance of Arcs	7×10^{10}	10^{10}	0.3×10^{10}	
Repetition Rate	180	60	5	Hz
Bunch Length σ_z in Linac	1.5	1.5	1.5*	mm
Normalized Transverse Emittance at End of Linac (Electrons)	3×10^{-5}	10×10^{-5}	$3\text{-}20 \times 10^{-5}$	mrad
Spot Radius at IP	1.6	2.8	—	Microns
Luminosity	6×10^{30}	6×10^{27}	—	cm^{-2} sec^{-1}

*Bunch length increases with current. At 1.2×10^{10}/bunch the bunch length is 1.5 mm in the linac.
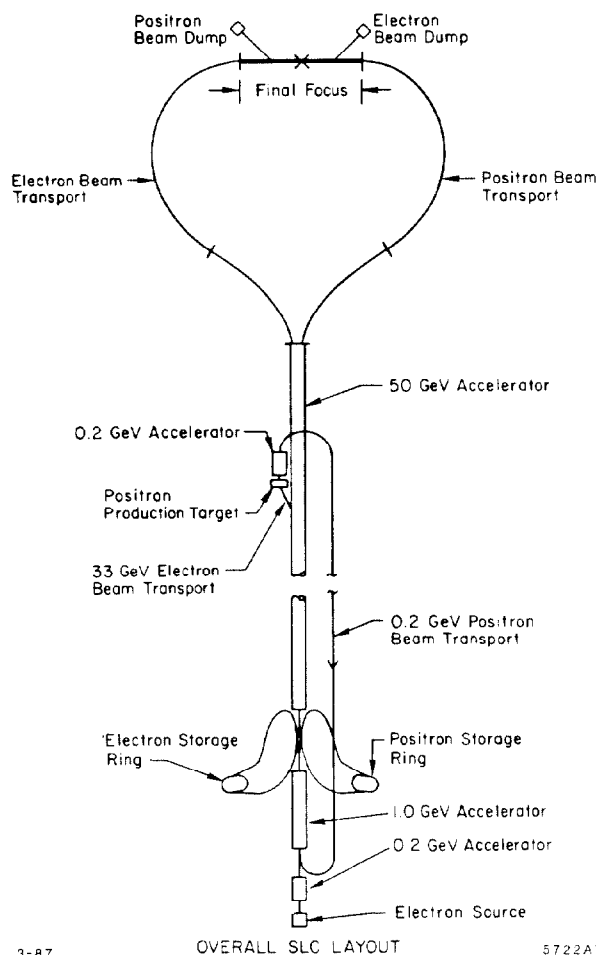
Figure 1

The beam transport lines between the storage rings and the accelerator are provided with sections of powered waveguide which are used to introduce a correlation between the energy of the particles in the bunches and the positions of the particles along the bunch. This correlation, in combination with the non-isochronous beam transport, causes the length of the bunches to be compressed from the equilibrium value in the storage rings (0.6 cm) to the length needed for acceleration in the linear accelerator (1.5 mm).

The positron bunch and the first electron bunch which follows it in the linac are accelerated to 51 GeV. The two bunches are separated at the high energy end of the accelerator and travel through beam transports which bring them into collision at the interaction point. After interacting, the bunches are deflected into beam dumps.

The second electron bunch accelerated in the linac is extracted at the 2/3 point of the linac, at an energy of 33 GeV, in order to produce positrons. The positrons are accelerated to 200 MeV and are returned to the injector end of the accelerator.

3. Status of Commissioning of the Major SLC Systems

Electron source and 1.2 GeV linear accelerator:

A schematic diagram of the electron (and positron) injector is shown in Fig. 2. The design goal for the electron injector is to provide two bunches of electrons with a population of 7.5×10^{10} each and a momentum spread of less than $\pm 1\%$ for injection at 1.2 GeV into the electron storage ring. The design goal for the transverse emittance of the bunches depends on the repetition rate of the linac. A lower repetition rate permits a longer time for synchrotron radiation damping in the storage ring. The specification for 180 Hz operation is a maximum transverse emittance of 30×10^{-5} mrad while the specification for 120 Hz operation is 180×10^{-5} mrad.

In the recent commissioning period bunch populations of 6×10^{10} have been present at 40 MeV and 5×10^{10} at 1.2 GeV at the injection septum of the electron storage ring. The energy spread specification has been met without difficulty under this operating condition. Up to now the commissioning has been conducted with the acceleration of a single bunch of electrons. When a faster rise time extraction kicker is installed in the electron storage ring it will be possible to accelerate two bunches of electrons. It is more difficult to maintain both bunches within

the 2% energy aperture of the storage ring because of the beam loading effect of the leading bunch on the trailing bunch. This compensation is accomplished by injecting the leading bunch into the accelerating structure before its peak voltage has been reached. Feedback has been developed to maintain the energy, energy difference, and energy spread of the pairs of electron bunches. The acceleration of two bunches with a population greater than 5×10^{10} each and with a combined energy spread of less than 2% has been demonstrated.

Transverse emittance measurements at 1.21 GeV are shown in Fig. 3. The point at 1.0×10^{11} particles is the combined emittance of two 5.0×10^{10} bunches accelerated simultaneously to 1.2 GeV. The emittance specification for 120 Hz operation has been met at bunch populations as large as 1×10^{11} while the emittance specification for 180 Hz operation has not been met consistently at bunch populations exceeding 4×10^{10}. Since the initial operation of the SLC will be at 120 Hz or 60 Hz, present electron beam emittance is adequate.
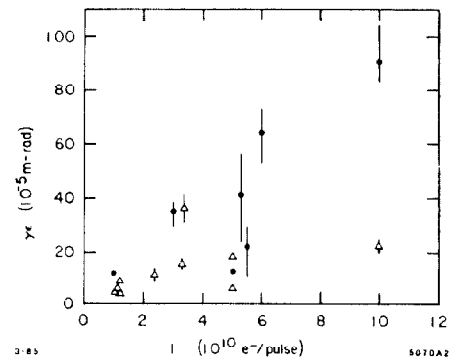
Fig. 3. Electron transverse emittance measurements at 1.21 GeV.

Storage Rings:

Two identical storage rings are part of the SLC design. These rings are used to damp the transverse emittance of positrons or electrons to meet the SLC invariant emittance specification of 3.0×10^{-5} mrad. The commissioning of the electron storage ring has been completed. A photograph of this ring is shown in Fig. 4. Figure 5 shows a measurement of the
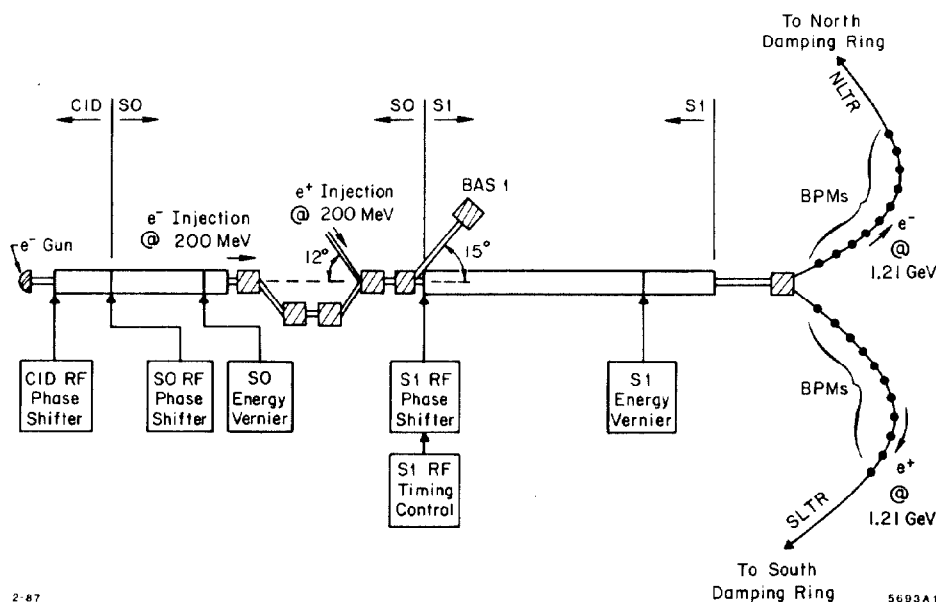
Fig. 2. Schematic view of the SLC 1.2 GeV Electron (and positron) injector.

2

transverse emittance of the extracted electron beam as a function of storage time. At the present time the SLC cannot operate at a repetition rate greater than 120 Hz (8.3 ms storage time) because of power limitations on the linac modulators. The electron storage ring easily meets the SLC specification for emittance at 120 Hz. To meet the SLC specification at 180 Hz it will be necessary to couple vertical and horizontal betatron motion to decrease the horizontal emittance after 53 ms.
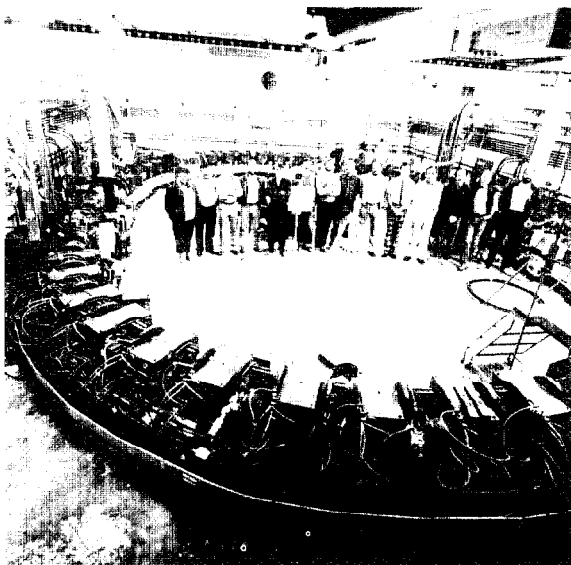

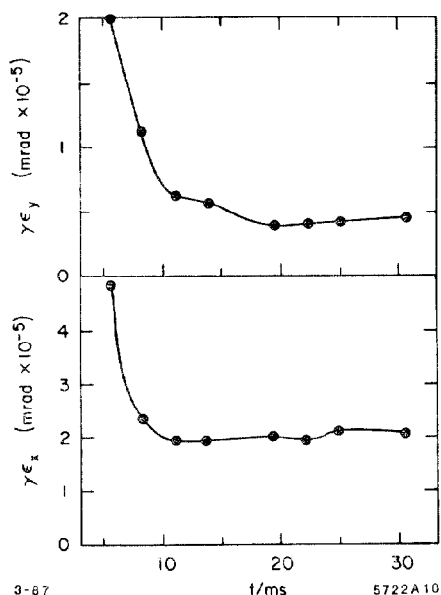Fig. 4. The SLC electron storage ring.

Fig. 5. The emittance of the beam extracted from the electron storage ring as a function of storage time. The vertical emittance $\gamma\epsilon_y$ is smaller than the horizontal emittance because the ring is operated without coupling.

The specification on the equilibrium RMS bunch length in the storage rings is 6 mm. The bunch compression system between the rings and the linac was designed to compress a 6 mm bunch to 0.5 mm. Figure 6 shows a measurement of the bunch length of the beam extracted from the electron ring. The increase with current of the bunch length was not anticipated in the design of the compression system. Because the storage ring bending magnets operate at a field of 2 Tesla an objective

of the initial design was to make the size of the vacuum chamber as small as possible. Recent calculations have indicated that the longitudinal impedance of the vacuum chamber is too large. There are many transitions where the shape of the vacuum chamber changes. Although an attempt was made in the original design to smooth these transitions, recent calculations show that the impedance reduction that was achieved was insufficient. Until the rings and compression system are modified it may not be possible to reach the SLC design luminosity. A plan of modifications is being developed at this time.
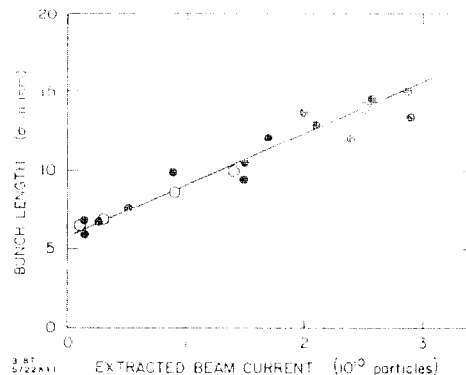

Fig. 6. The bunch length (σ_z) of the beam extracted from the electron storage ring.

The SLC specification calls for the simultaneous injection and extraction of two electron bunches separated by about half a ring circumference. The difficulty of constructing the injection and extraction kickers was not appreciated at the time the rings were designed. The space allowed for the kicker magnets turned out to be too small for magnets that could be constructed easily and the first kicker design did not meet the required specifications. A new kicker system has been designed and the first example constructed has been installed as the injection kicker. Two bunches with a population greater than 1×10^{10} electrons each have been injected into the ring. A kicker suitable for extraction is being constructed now. Until this kicker is installed and successfully commissioned, the SLC will have to operate in a mode in which only one bunch of electrons is present in the storage ring at any time. In this mode, collisions at the interaction point will occur on every other linac pulse.

The positron storage ring was commissioned with electrons. The polarity of this ring was recently reversed and the commissioning with positrons has just begun. A positron bunch population of 4×10^9 has been achieved.

50 GeV Linear Accelerator:

In order to achieve the energy gradient required for SLC operation it was necessary to design and produce a new higher power klystron. This klystron is known as the 5045 and it replaces the previously installed XK5 klystrons. This new klystron operates with a peak power output of about 67 MW and a pulse length of 3.5 μs. The original specification of the new klystron was 50 MW and 5.0 μs. Midway along in the installation of new klystrons it was found that the new klystron had a better energy efficiency when operated at a higher peak power and a shorter pulse length. All of the klystrons that were not yet installed were provided with pulse transformers with a higher step-up ratio in order to accommodate the new operating condition.

The principal difficulties which were encountered in the production of the new klystron were window breakage, cathode gas emission, and microwave instability. Despite a considerable effort, no single window solution was found. The

3

output power from the klystron is now split in half and directed through two windows and then is recombined. Window breakage is now a very infrequent event. The emission of gas from the cathodes has been eliminated by altering the cathode manufacturing procedures. Finally, a beam breakup instability has been improved by small changes in the klystron cavities. The present yield for producing a satisfactory klystron from parts in the SLAC factory is greater than 75%.

The linac is now equipped with 200 of the new klystrons and 44 of the old klystrons. The average energy gain provided by 40 feet of accelerating structure powered by one of the new klystrons is 240 MeV. Over one million operating hours have been accumulated, mostly at a repetition rate of 10 Hz. The cathode lifetime is now projected to be greater than 40,000 hours and the mean time between failures is now about 18,000 hours and is rising.

Higher gradients in the accelerating structure have not been troublesome. There are locations in the accelerator where one klystron drives two accelerator sections rather than four. Even these sections function satisfactorily. It was necessary, however, to replace the original waveguide valves. This valve, which must pass microwaves when open, serves to make a vacuum seal when closed. The old valve could not handle the higher power levels of the new klystrons without arcing.

Space charge forces within the accelerating waveguide are very large. In order to keep transverse wake fields from displacing the phase space of the trailing part of the bunch from the phase space of the head of the bunch, strong focusing and accurate beam centering within the linac irises is necessary. The SLC design calls for an RMS beam centering error of 100 microns or less. Figure 7 shows horizontal and vertical beam positions through the linac that are typical of recent operation. The RMS error is 200 microns. Figure 8 is the profile of the electron beam at 47 GeV. The profile has a small tail caused by wake fields and a residual shape from mismatch from compression in the transfer line between the storage ring and the linac. Figure 9 shows a profile when the beam in the linac is not carefully centered in the irises. The tails contain a larger proportion of the charge than when the beam is centered in the irises.

Table 2 shows a summary of invariant emittance measurements made at various distances along the linac. The vertical emittance meets the SLC design specification of 3×10^{-5} mrad at bunch populations up to 1×10^{10}. The horizontal emittance is somewhat larger. It is believed that this difference results from residual dispersion present at the injection point in the linac where the horizontally-bending beam transport between the storage ring and the linac are joined.
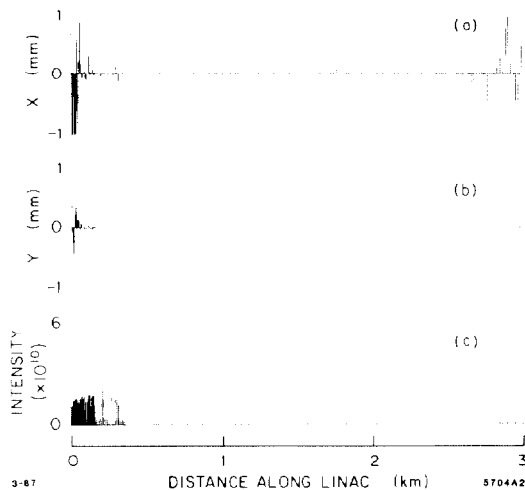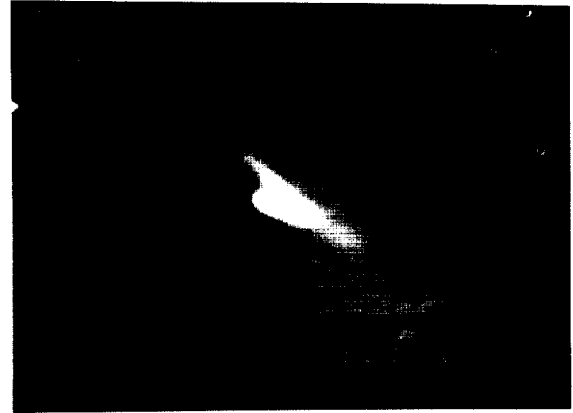

Fig. 8. Electron beam profile at 47 GeV. The small tail is caused by transverse wake fields. The core of the spot is about 100μ in diameter.
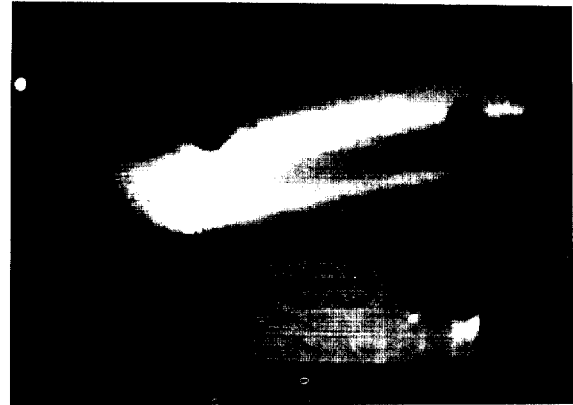

Fig. 9. Electron beam profile of a poorly steered beam. Large tails are evident.

Table 2. Summary of Transverse Emittance Measurements
Invariant emittance in units of 1×10^{-5} mrad.
I is in units of 1×10^{10} and E in GeV.

Location in Linac	I	E	$\gamma\epsilon_x$	$\gamma\epsilon_y$
Ring Exit	2	1.2	2.2 ± 0.3	0.4 ± 0.1
0 Km	2	1.2	13 ± 3	1.3 ± 0.3
1 Km	0.7	8.5	8 ± 1	
1 Km	1.5	8.5	11 ± 2	2.5 ± 0.3
3 Km	0.4	43	7 ± 1	
3 Km	0.8	47	12 ± 4	1.1 ± 0.3
3 Km	1.0	34	25 ± 5	2.1 ± 1.0
3 Km	1.5	43	20 ± 5	4 ± 1

At bunch populations below 1×10^{10} it is routinely possible to maintain a total energy spread in the beam of less than 0.4%. When larger populations are accelerated, the energy spread increases because of the bunch lengthening in the storage ring. It is intended to maintain the energy and energy spread of the linac beams constant by the use of feedback systems. Figure 10 shows the open loop energy error for electrons detected at 47 GeV over two-minute intervals. Figure 10(a) shows the effect of a faulting klystron. The faulting klystron was removed from the beam before the data of Fig. 10(b) were taken. The rms energy jitter is less than 0.13% in Fig. 10(b).
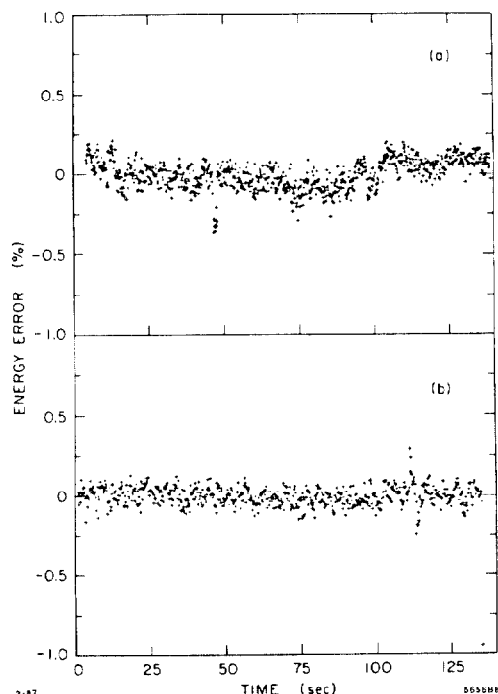

Fig. 7. Horizontal (X) and vertical (Y) beam positions measured along the linear accelerator.

4

Figure 10

Figure 12

Positron Source:

A schematic diagram of the SLC positron production system is shown in Fig. 11. Figure 12 shows the positron production target and the first magnetic focusing element in the system. Typical recent performance figures for the positron source are shown in Table 3. More than 1.5 positrons are
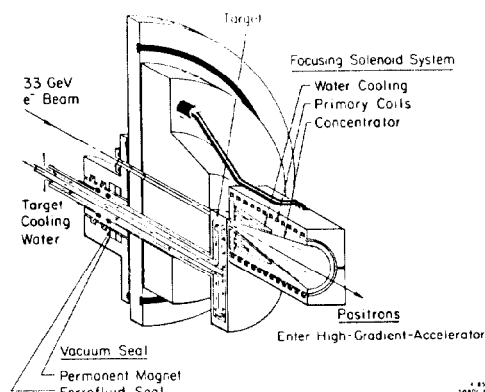
present in the momentum-analyzed 200 MeV return line beam for every electron incident on the positron production target.

The presently installed positron source hardware is not operating at the design specification parameters. In particular, the solenoidal focusing throughout the system is operating at from 0.6 to 0.75 of the design values. Furthermore, the accelerating gradient in the section where the positrons are captured into RF buckets is operating at 0.5 of the design value. Finally, the channel in the septum where the electrons are extracted from the linac contains a partially collapsed vacuum chamber. All of the components that are not operating according to specification will be replaced in May. When these changes are made, it is expected that the positron yield will double.

The positron bunch length is a very important parameter because the positrons must be accelerated to 1.2 GeV in a 2856 MHz linac. Since the momentum acceptance of the positron storage ring is only 2%, the positron bunch length must be less than 6 mm total. A Cerenkov radiator coupled to a streak camera is used to measure the bunch length. A recent study of the bunch length and yield as a function of capture-RF-section phase is shown in Fig. 13. It is intended to also use the two 180 degree bends in the positron system to compress the bunch length. A considerable contribution to the positron bunch length is the bunch length of the electron beam used to produce the positrons. Until the bunch length-ening problem in the electron storage ring is corrected, some of the positrons produced may not be accepted in the positron storage ring because they will have too large an energy spread.

4. Beam Transport Between the Linac and the Final Focus

A very high gradient beam transport system ($n = 32824$) is used between the linac and the final focus. Strong gradients are used to suppress the emittance growth caused by quantum fluctuations in the emission of synchrotron radiation. Figure 14 shows a schematic cross section of the beam transport magnets. Because the gradients are high, it was necessary to survey the
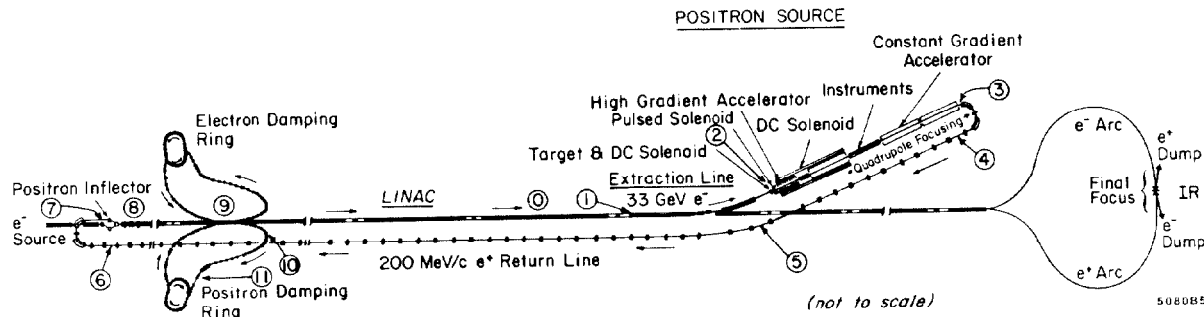
Table 3. Recent Performance Figures for the SLC Positron System

Beam	Intensity ($\times 10^{10}$)	Yield	Location Micro	Unit	
e^-	0.	2.6		LI10	133	Linac Sector 10
	1.	2.2		EP01	175	Extraction Line After Septa
	2.	2.0	=1	EP01	335	Targeted e^- Beam
e^+	3.	4.4	2.2	EP02	631	Captured Positrons Before Momentum Analysis
	4.	3.2	1.6	EP02	812	At 190 MeV, After East Turn
	5.	3.2	1.6	LI19	1152	At Beginning of Return Line
	6.	3.0	1.5	LI01	2952	Before West Turn
	7.	2.9	1.5	EP05	3152	After West Turn
	8.	2.6	1.3	LI01	141	Linac Beginning of Sector 1
	9.	1.8	0.9	LI01	835	End of Sector 1
	10.	1.7	0.85	DR01	241	Into SLTR Transport
	11.	1.0	0.5			SLTR Faraday Cup

Fig. 11. Schematic diagram of the positron source.

5

magnets into place with 100 micron accuracy. The survey task was complicated by the fact that the high gradient transport is not all in one plane. It is steeply contoured to follow the slope of the site on which the SLC is constructed. Initial tests with beam indicate that the survey tolerances were achieved.

Beam trajectory correction is accomplished with a system of beam position monitors and mechanical magnet movers. An electron beam has been transported from the end of the linac to the final focus. Initial work on trajectory correction has begun. Figure 15 shows the beam position monitor reading throughout the electron transport at a time when only enough magnets had been moved to achieve transmission of the beam through the system. Work to adjust the magnet positions in order to achieve the specified 100 micron beam centering tolerance is in progress.
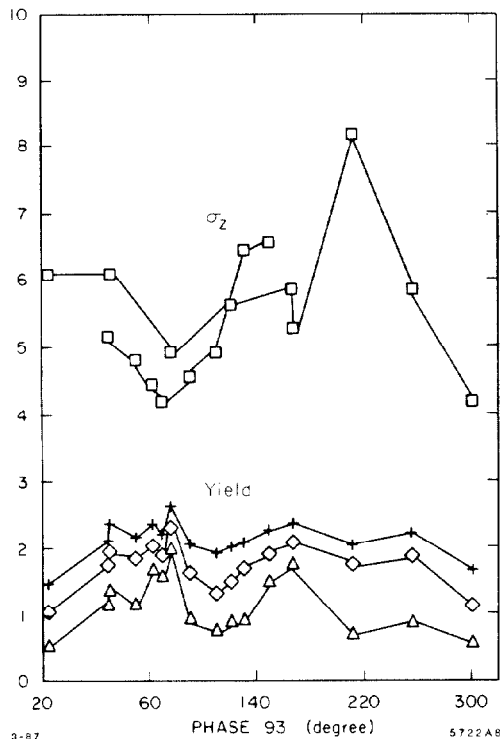

Fig. 13. Positron yield and bunch length as a function capture-RF-section phase.
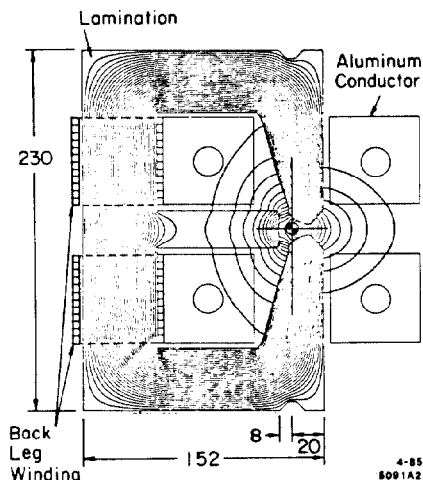

Fig. 14. A Cross section of the high gradient beam transport magnets. The dimensions are given in millimeters.
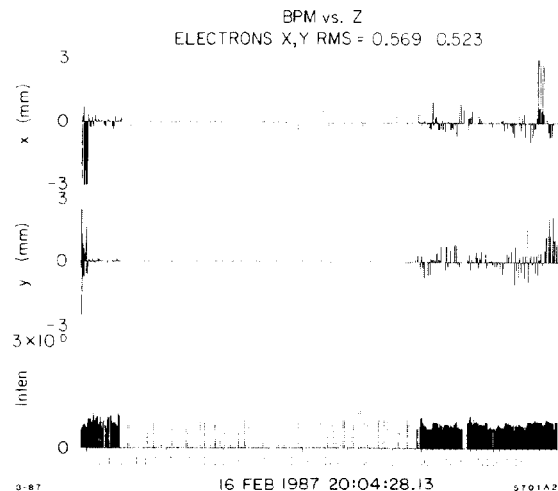

Fig. 15. Beam position monitor data taken shortly after the electron beam was first transmitted to the final focus. The bottom scale is a rough intensity measurement.

5. Final Focus

The final focus optical system is designed to produce a chromatically corrected 1.7 mrad beam spot at the interaction point. When the momentum of the incident beam is within $\pm 0.5\%$ of the design value, the optical system produces a beta value at the interaction point of 0.75 cm. A schematic diagram of this optical system is shown in Fig. 16.

In an initial test lasting only a few hours electrons were transmitted through the north portion of the final focus to a stopper 20 meters from the interaction point without major steering corrections. A program to transmit the electron beam across the interaction point is now in progress. This program will consist of steering and focussing corrections to adjust the system to produce the design spot size at the interaction point.

A 7 micron diameter movable wire has been installed at the interaction point to measure the beam profile. When beam profiles that are smaller than the wire diameter have been achieved the 7 micron wire will be replaced with a 4 micron wire. After the optical elements have been adjusted to produce a small beam spot, the beams will be brought into collision through the use of a precision beam position monitor at the interaction point. This monitor has sufficient accuracy to bring the beams to within 10 microns of each other. When the beams are separated by less than 40 microns the steering effect of one beam on the other can be detected with other beam position monitors. The steering effect, which vanishes when the beams collide head on can be used to center the beams with an accuracy of better than one quarter of their transverse dimension. Finally, detectors have been constructed to observe synchrotron radiation emitted during the collisions. The synchrotron radiation strength will be used to reduce the spot size below that which can be resolved with the 4 micron wire.
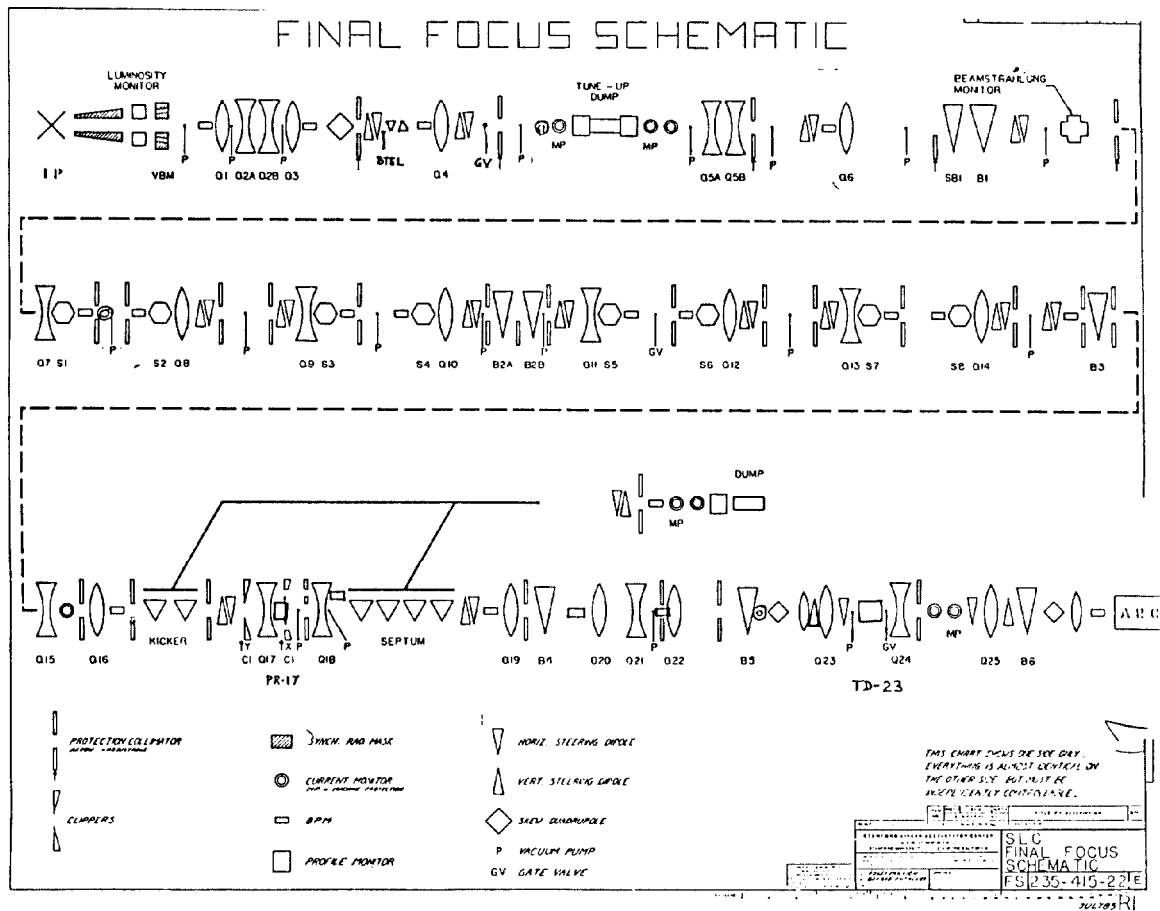
6

FINAL FOCUS SCHEMATIC

Figure 16

7

PAC 1987